Martian subsurface volatile concentrations as a function of time: Clues from layered ejecta craters

Nadine G. Barlow

Department of Physics and Astronomy, Northern Arizona University, Flagstaff, Arizona, USA

Received 14 November 2003; revised 26 January 2004; accepted 5 February 2004; published 5 March 2004.

[1] Martian layered ejecta morphologies are characterized using a new preservation classification system and through measurement of ejecta mobility (EM) ratios. EM, the ratio of ejecta extent to crater radius, is believed to provide information about ejecta material fluidity during emplacement. This study compares EM and preservation classification to determine if subsurface volatile concentrations have changed measurably over time. Results from both regional and local analyses suggest that concentrations of subsurface volatiles have remained approximately constant at the depths and over the time periods recorded by these craters. *INDEX TERMS:* 5415 Planetology: Solid Surface Planets: Erosion and weathering; 5420 Planetology: Solid Surface Planets: Impact phenomena (includes cratering); 5464 Planetology: Solid Surface Planets: Remote sensing; 5470 Planetology: Solid Surface Planets: Surface materials and properties. **Citation:** Barlow, N. G. (2004), Martian subsurface volatile concentrations as a function of time: Clues from layered ejecta craters, *Geophys. Res. Lett.*, *31*, L05703, doi:10.1029/2003GL019075.

1. Introduction

[2] Most fresh Martian impact craters are surrounded by a layered/fluidized ejecta pattern, which can be characterized as single layer (SLE), double layer (DLE), or multiple layer (MLE) based on the number of ejecta layers observed [*Barlow et al.*, 2000]. Layered morphologies are proposed to result from vaporization of subsurface volatiles [*Carr et al.*, 1977; *Greeley et al.*, 1980; *Wohletz and Sheridan*, 1983; *Stewart et al.*, 2001; *Baratoux et al.*, 2002] or by interactions with Mars' thin atmosphere [*Schultz and Gault*, 1979; *Barnouin-Jha and Schultz*, 1998; *Barnouin-Jha et al.*, 1999a, 1999b]. Analysis of diameter-latitude-morphology relationships [*Costard*, 1989; *Barlow and Bradley*, 1990], correlation with other morphologic features indicative of subsurface volatiles [*Costard and Kargel*, 1995; *Carr*, 1996], and hydrocode simulations of impacts into volatile-rich targets [*Stewart et al.*, 2001] strongly support the subsurface volatile model for layered ejecta formation on Mars [*Boyce and Roddy*, 1997].

[3] Ejecta mobility (EM) ratio quantifies the distance to which ejecta material extends beyond the crater rim [*Mouginis-Mark*, 1979, 1981; *Costard*, 1989]:

$$\mathrm{EM} = (\text{maximum extent of ejecta})/(\text{crater radius})$$

EM is believed to provide constraints on the degree of material fluidity at the time of ejecta emplacement, and thus likely provides information about target material volatile concentration during crater formation. Variations in EM occur among ejecta morphology type and with location, suggesting that volatile concentrations vary [*Mouginis-Mark*, 1979, 1981; *Costard*, 1989; *Barlow and Pollak*, 2002]. EM variations with location are consistent with proposed distributions of subsurface volatiles from geothermal considerations [*Clifford*, 1993] and Mars Odyssey Neutron Spectrometer results [*Feldman et al.*, 2002].

[4] Terrestrial debris flow studies indicate that a critical volatile concentration is necessary to initiate flow. Particle sizes and nature of the target material influence this critical concentration. *Woronow* [1981] found critical water concentrations of ~16% using finite element modeling to estimate volatile content of clay-rich rampart (layered ejecta terminating in a distal ridge) ejecta deposits. Hydrocode simulations suggest ~20% volatile concentration is required to initiate flow for Martian SLE craters [*Stewart et al.*, 2001]. Unfortunately no studies have been conducted which describe how changes in volatile concentration affect ejecta deposit extent. Thus, this study focuses on qualitative implications of ejecta extent observations rather than estimating quantitative constraints on volatile contents of subsurface reservoirs.

[5] EM could indicate how subsurface volatile concentration has changed over time if we could determine the relative ages of individual craters. Such age relationships have been difficult to derive because of spatial and temporal variations in degradation processes operating on Mars. Also, Viking imagery, our primary source of information until recently, provided only qualitative estimates of crater degradation. New topographic and infrared data for Mars allow us to now obtain morphometric and thermophysical measurements which can help constrain the preservational state of individual craters. Mars Global Surveyor (MGS) Mars Orbiter Laser Altimeter (MOLA) data allow us to compare a crater's morphometric characteristics (crater depth, rim height, etc.) to those expected for a fresh crater of similar size to determine the amount of degradation experienced by the crater. Mars Odyssey (MO) Thermal Emission Imaging System (THEMIS) (100 m/pixel resolution) provides day and night infrared imagery which constrains dust versus rock concentrations. Combined with higher resolution visible imagery provided by MGS Mars Orbiter Camera (MOC) (up to 2 m/pixel resolution) and MO THEMIS Visible camera (THEMIS VIS; 18 m/pixel resolution), we can develop a relative preservation classification system for individual craters on Mars. Comparing a crater's preservation class with its EM

0094-8276/04/2003GL019075

Table 1. Preservation Classification

Class	Relative Depth[a]	Rim	Ejecta	Interior	Relative TI[b]	Rank Range
0.0	~0 (0)	Rimless (0)	None (0)	None (0)	Same (0)	0
1.0	<1/4 (1)	Rimless (0)	None (0)	Flat floor/Floor deposits (1)	Same (0)	1–2
2.0	1/4 to 1/2 (2)	Rimless (0)	None (0)	Flat floor/Floor deposits (1)	Same (0)	3–4
3.0	1/4 to 1/2 (2)	Slightly elevated (1)	None (0)	Highly Degraded (2)	Same (0)	5–7
4.0	1/2 to 3/4 (3)	Rounded, elevated (2)	Barely Discernible (1)	Moderate Degradation (3)	Same (0)/slightly higher (1)	8–11
5.0	1/2 to 3/4 (3)	Slight degradation (3)	Moderate erosion (2)	Slight Degradation (4)	Slightly higher (1)	12–15
6.0	>3/4 (4)	Sharp (4)	Slight erosion (3)	Slight Degradation (4)	Higher (2)	16–18
7.0	~1 (5)	Sharp (4)	Pristine (4)	Pristine (5)	Higher (2)	19–20

[a]Relative depth is the current depth of the crater compared to the depth expected for a fresh crater of similar size. Depth is measured from the surrounding terrain level to the deepest part of the crater floor.

[b]Relative TI is the thermal inertia of the crater ejecta region compared to the surroundings. "Same" indicates that the TI of the ejecta region is less than a factor of 1.25 times as high as the average TI of the surrounding material. "Slightly higher" is assigned to ejecta regions whose TI is between 1.25 and 2 times higher than the surrounding material. "Higher" indicates that the TI of the ejecta region is >2 times the average value of the surroundings.

Values in parentheses in each column indicate the numerical ranking for a feature with that characteristic. These rankings are used to determine the crater's final preservation class, as indicated in the final column. The ranking range is adjusted if a particular column of data is unavailable for a crater.

value allows us to determine if subsurface volatile concentrations have varied measurably over time.

2. Methodology

[6] We developed an 8-point preservation classification system using Viking, MOC, THEMIS VIS, THEMIS IR, and MOLA data. A numerical ranking is given for different values of relative crater depth (distance between crater floor and surrounding terrain, determined from MOLA digital elevation models), rim sharpness, ejecta blanket preservation, interior feature(s) preservation, and thermal inertia (TI) of ejecta compared to surroundings. Summing these individual rankings determines a crater's preservational state (Table 1 and Figure 1). On this scale, 0.0 represents a "ghost crater" while 7.0 indicates an extremely fresh crater. Ejecta blankets are only seen for craters in preservational classes 4 through 7.

[7] This study includes all rampart craters $\geq$5-km-diameter in the MC08, 09, 10, 11, 15, 16, 17, 18, and 19 quadrangles. The regions cover both younger plains materials and older highlands units within the Martian equatorial zone, where temporal variations in subsurface volatile content are expected to be most obvious. Only SLE craters (believed to result from impact into subsurface ice reservoirs) are included because their large numbers and widespread distribution provide the best statistics [*Barlow and Perez*, 2003]. Only rampart craters were included since the number of non-rampart craters in the study area was too small to provide statistically significant results.

[8] We investigated EM versus preservation trends for both local and regional areas which are mapped as the same geologic unit or as geologic units of the same stratigraphic age [*Scott and Tanaka*, 1986; *Greeley and Guest*, 1987]. This limitation reduces the effects of regional erosion variations. Local areas are a single geologic unit within an individual quadrangle. Regional areas consist of the same geologic unit over its entire regional extent. We also combined data from all craters on units of the same stratigraphic age to improve statistics. We averaged EM values for all craters of the same preservation class. Figure 2 shows example results for local and regional areas. Figure 3 shows results for craters on all units of the same stratigraphic age across the study area.

3. Results and Implications

[9] Older craters (preservation classes 4.0–4.5) often display lower EM than younger craters (higher preservation classes). This is consistent with degradation processes affecting ejecta blankets of the older craters. Craters in classes 5.0 to 7.0 typically do not display any statistically significant differences in EM over either local or regional areas.

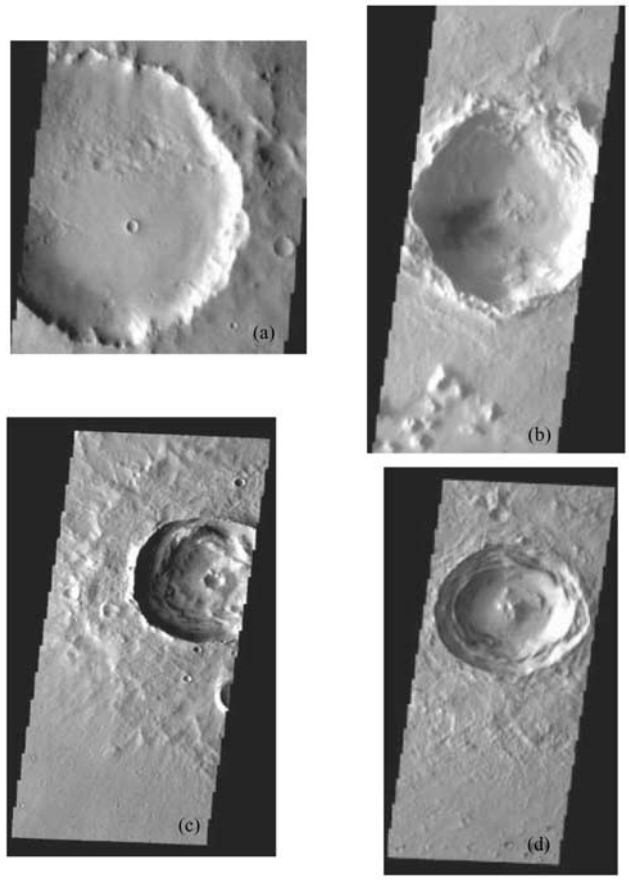

Figure 1. Example Craters of Various Preservation Classes. (a) Preservation class 2.0. Crater is 18 km in diameter and located at 10.2°N 17.2°E (THEMIS image V06503024). (b) Preservation class 4.0. Crater is 21.5 km in diameter and located at 13.2°N 167.5°E (THEMIS image V05986005). (c) Preservation class 6.0. Crater is 14 km in diameter and located at 11.9°N 300.7°E (THEMIS image V06256020). (d) Preservation class 7.0. Crater is 16.5 km in diameter and located at 12.6°N 83.8°E (THEMIS image V05914015).

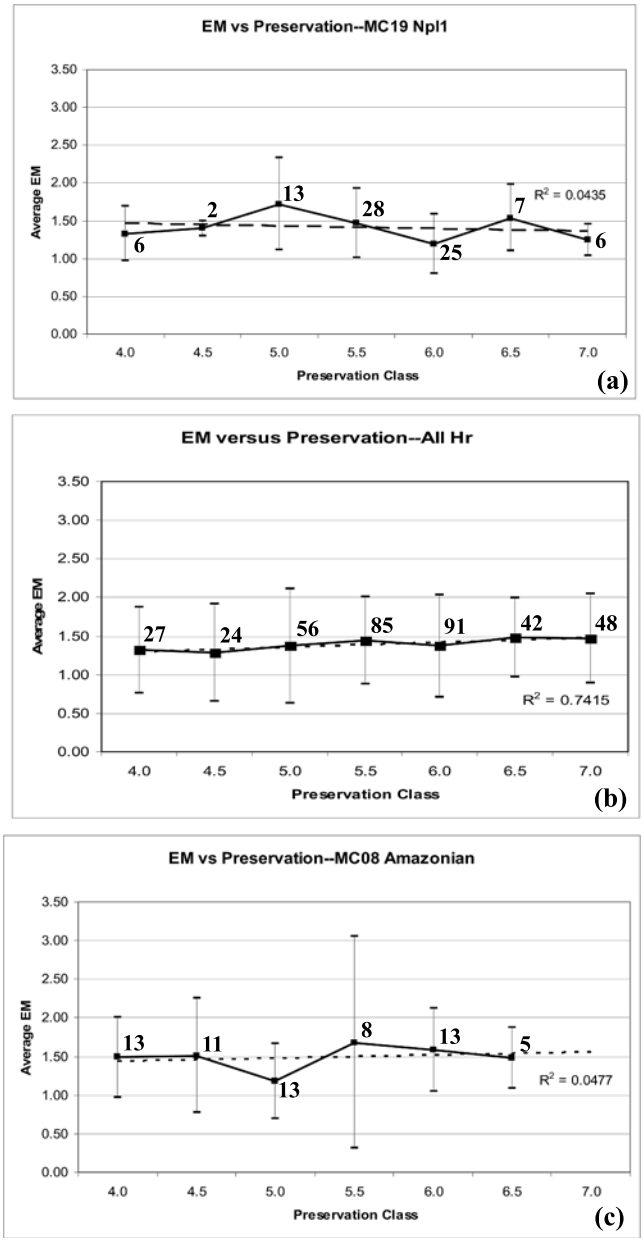

Figure 2. EM versus Preservation Class for Local and Regional Areas. Dashed lines show the least-squares fit trendlines to the data. In all three cases, no statistically significant variation in average EM with crater preservational age is seen. Error bars are one standard deviation and the numbers next to the data points are the number of craters in each preservation class. (a) Graph showing the average EM as a function of preservation class for all units classified as the Npl_1 stratigraphic unit within the MC19 quadrangle (local area). (b) Graph showing average EM versus preservation class for all Hr stratigraphic units within the study area (regional area). (c) EM versus preservation class for all Amazonian-aged stratigraphic units within the MC08 quadrangle (local area).

[10] Average EM over all preservation classes does not vary significantly by terrain and the differences are not statistically significant (Figure 3). Crater size-frequency distribution analyses indicate that craters retaining ejecta blankets formed within the post-heavy bombardment period (approximately the past 3.5×10^9 years) [*Barlow*, 1990].

[11] There are two possible explanations for these results:

[12] (1) The concentration of subsurface volatiles has not changed over time or has not changed enough to be detected

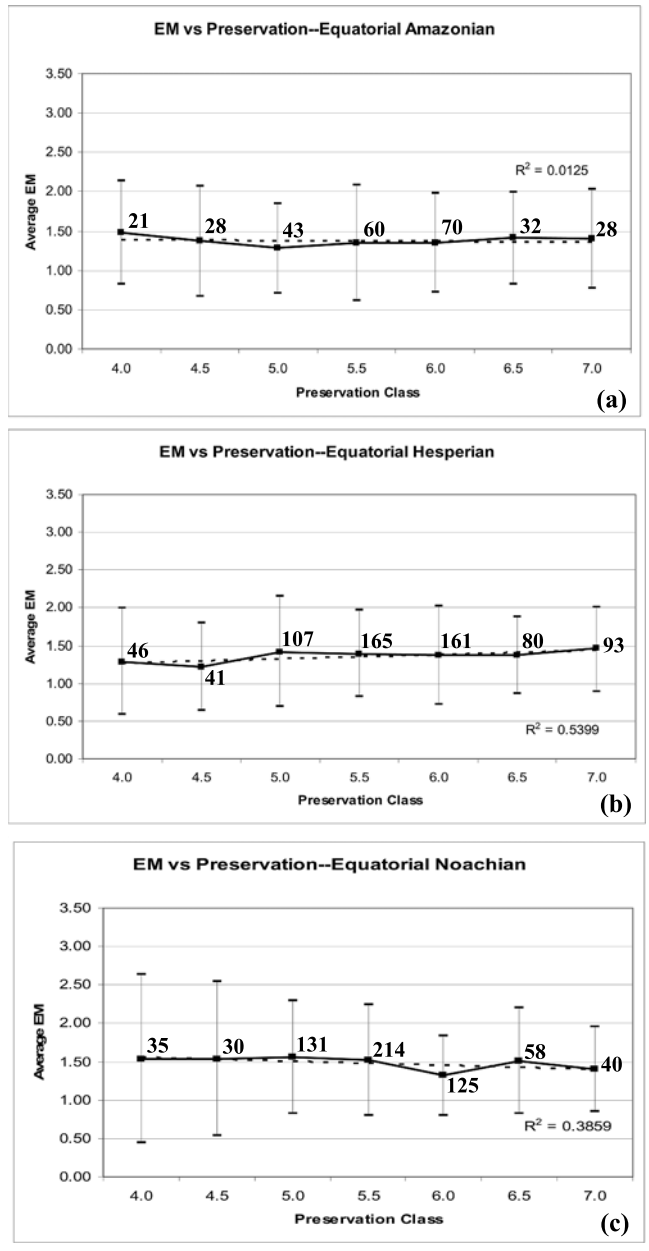

Figure 3. EM versus Preservation Class by Stratigraphic Unit. Dashed lines represent the least-squares fit trendline to the data and errors are one standard deviation. Numbers next to the data points are the number of craters in each preservation class. Results suggest that no statistically significant change in average EM occurs over the time periods recorded by the craters on these units. (a) Average EM versus preservation for all Amazonian-aged stratigraphic units in study area. (b) Average EM as a function of preservation for all Hesperian-aged stratigraphic units in study region. (c) Average EM versus preservation for all Noachian-aged stratigraphic units in the equatorial study area.

through this type of analysis. Modeling by *Mellon and Jakosky* [1995] found that volatile reservoirs deeper than 2 meters should not be affected by diurnal, seasonal, or long-term temperature variations over at least the past 2.5×10^6 yrs. Depth-diameter relationships derived from MOLA topography [*Garvin et al.*, 2003] and theoretical considerations [*Melosh*, 1989] suggest our smallest craters are excavating to depths of at least 770 m, well below the region which is affected by temperature variations. However, the total concentration of volatiles necessary to produce the observed EM values is not well constrained. Our results imply that volatile concentrations apparently have not dropped below ~16–20% (critical volatile concentrations found by *Woronow* [1981] and *Stewart et al.* [2001]) and likely have not varied by an extreme amount over the times considered.

[13] (2) The layered ejecta morphologies result from interactions of the ejecta curtain with the Martian atmosphere and tell us nothing about subsurface volatiles. Ejecta interaction with Mars' thin atmosphere is another proposed mechanism for producing layered ejecta morphologies. Those models suggest that particle size rather than volatile concentration is the primary determinant of EM and sinuosity values for SLE craters [*Barnouin-Jha and Schultz*, 1998]. These results alone would be consistent with no long-term changes in Martian atmospheric density over the proposed time scale, but many other lines of evidence suggest that subsurface volatiles are the dominant contributor to layered ejecta morphologies and their characteristics [*Boyce and Roddy*, 1997]. As such, we believe our results are better explained by the first hypothesis.

[14] Results of this analysis combined with the *Mellon and Jakosky* [1995] models suggest that, within statistical uncertainties, subsurface volatile concentrations have been relatively stable over at least the past 3.5×10^9 years on Mars. Observed differences in EM values therefore provide information on actual regional variations in subsurface volatile concentrations at depths >700 m, which likely persist to the present day in most areas of Mars.

[15] **Acknowledgments.** The author thanks Joseph Boyce and a second reviewer for constructive comments which substantially improved the manuscript. This study was funded through NASA Mars Data Analysis Program Grant NAG5-12510.

References

Baratoux, D., D. Delacourt, and P. Allemand (2002), An instability mechanism in the formation of the Martian lobate craters and the implications for the rheology of ejecta, *Geophys. Res. Lett.*, *29*(8), 1210, doi:10.1029/2001GL013779.

Barlow, N. G. (1990), Constraints on early events in Martian history as derived from the cratering record, *J. Geophys. Res.*, *95*, 14,191–14,201.

Barlow, N. G., and T. L. Bradley (1990), Martian impact craters: Correlations of ejecta and interior morphologies with diameter, latitude, and terrain, *Icarus*, *87*, 156–179.

Barlow, N. G., and C. B. Perez (2003), Martian impact crater ejecta morphologies as indicators of the distribution of subsurface volatiles, *J. Geophys. Res.*, *108*(E8), 5085, doi:10.1029/2002JE002036.

Barlow, N. G., and A. Pollak (2002), Comparisons of ejecta mobility ratios in the Northern and Southern Hemispheres of Mars, *Lunar Planet. Sci. [CD-ROM]*, *XXXIII*, abstract 1322.

Barlow, N. G., J. M. Boyce, F. M. Costard, R. A. Craddock, J. B. Garvin, S. E. H. Sakimoto, R. O. Kuzmin, D. J. Roddy, and L. A. Soderblom (2000), Standardizing the nomenclature of Martian impact crater ejecta morphologies, *J. Geophys. Res.*, *105*, 26,733–26,738.

Barnouin-Jha, O. S., and P. H. Schultz (1998), Lobateness of impact ejecta deposits from atmospheric interactions, *J. Geophys. Res.*, *103*, 25,739–25,756.

Barnouin-Jha, O. S., P. H. Schultz, and J. H. Lever (1999a), Investigating the interactions between an atmosphere and an ejecta curtain: 1. Wind tunnel tests, *J. Geophys. Res.*, *104*, 27,105–27,115.

Barnouin-Jha, O. S., P. H. Schultz, and J. H. Lever (1999b), Investigating the interactions between an atmosphere and an ejecta curtain: 2. Numerical experiments, *J. Geophys. Res.*, *104*, 27,117–27,131.

Boyce, J. M., and D. J. Roddy (1997), Martian crater ejecta, emplacement and implications for water in the subsurface, *Lunar Planet. Sci.*, *XXVIII*, 145–146.

Carr, M. H. (1996), *Water on Mars*, 229 pp., Oxford Univ. Press, New York.

Carr, M. H., L. S. Crumpler, J. A. Cutts, R. Greeley, J. E. Guest, and H. Masursky (1977), Martian impact craters and emplacement of ejecta by surface flow, *J. Geophys. Res.*, *82*, 4055–4065.

Clifford, S. M. (1993), A model for the hydrologic and climatic behavior of water on Mars, *J. Geophys. Res.*, *98*, 10,973–11,016.

Costard, F. M. (1989), The spatial distribution of volatiles in the Martian hydrolithosphere, *Earth Moon Planets*, *45*, 265–290.

Costard, F. M., and J. S. Kargel (1995), Outwash plains and thermokarst on Mars, *Icarus*, *114*, 93–112.

Feldman, W. C., et al. (2002), Global distribution of neutrons from Mars: Results from Mars Odyssey, *Science*, *297*, 75–78.

Garvin, J. B., S. E. H. Sakimoto, and J. J. Frawley (2003), Craters on Mars: Global geometric properties from gridded MOLA topography, paper presented at 6th International Conference on Mars, Lunar Planet. Inst., Houston, Tex.

Greeley, R., and J. E. Guest (1987), Geologic map of the eastern equatorial region of Mars, scale: 1:15,000,000, *USGS Misc. Invest. Map*, *I-1802-B*.

Greeley, R., J. Fink, D. E. Gault, D. B. Snyder, J. E. Guest, and P. H. Schultz (1980), Impact cratering in viscous targets: Laboratory experiments, in *Proceedings of the 11th Lunar Planetary Science Conference*, pp. 2075–2097, Pergamon, New York.

Mellon, M. T., and B. M. Jakosky (1995), The distribution and behavior of Martian ground ice during past and present epochs, *J. Geophys. Res*, *100*, 1781–1799.

Melosh, H. J. (1989), *Impact Cratering: A Geologic Process*, 245 pp., Oxford Univ. Press, New York.

Mouginis-Mark, P. (1979), Martian fluidized crater morphology: Variations with crater size, latitude, altitude, and target material, *J. Geophys. Res.*, *84*, 8011–8022.

Mouginis-Mark, P. (1981), Ejecta emplacement and modes of formation of Martian fluidized ejecta craters, *Icarus*, *45*, 60–76.

Schultz, P. H., and D. E. Gault (1979), Atmospheric effects on Martian ejecta emplacement, *J. Geophys. Res.*, *84*, 7669–7687.

Scott, D. H., and K. L. Tanaka (1986), Geologic map of the western equatorial region of Mars, scale: 1:15,000,000, *USGS Misc. Invest. Map*, *I-1802-A*.

Stewart, S. T., J. D. O'Keefe, and T. J. Ahrens (2001), The relationship between rampart crater morphologies and the amount of subsurface ice, *Lunar Planet. Sci. [CD-ROM]*, *XXXII*, abstract 2092.

Wohletz, K. H., and M. F. Sheridan (1983), Martian rampart crater ejecta: Experiments and analysis of melt-water interactions, *Icarus*, *56*, 15–37.

Woronow, A. (1981), Preflow stresses in Martian rampart ejecta blankets: A means of estimating the water content, *Icarus*, *45*, 320–330.

N. G. Barlow, Department of Physics and Astronomy, Northern Arizona University, NAU Box 6010, Flagstaff, AZ 86011-6010, USA. (nadine.barlow@nau.edu)